International Prediction Event on the Behavior of Bored, CFA and Driven Piles in ISC'2 Experimental Site – 2003

Prediction of the behavior of a pile foundation under static loading condition using in situ test results

Nelson Aoki
José Carlos A. Cintra
Edmundo Rogério Esquivel
Luiz Russo Neto

University of São Paulo at São Carlos
Geotechnical Engineering Department
Brazil

Prediction of behavior of a pile foundation under static loading condition using in situ test results

1 Definition

An isolated pile foundation is a system composed of a structural pile element embedded in soil layers around the pile shaft and the soil layers between the pile base and the reference surface beneath the pile base. Reference surface is defined as the surface below which the soil deformation due to foundation loads can be neglected. Predicted pile settlement is a vector that measures the distance variation between the pile head (where the load is applied) and the reference surface.

2 Pile location

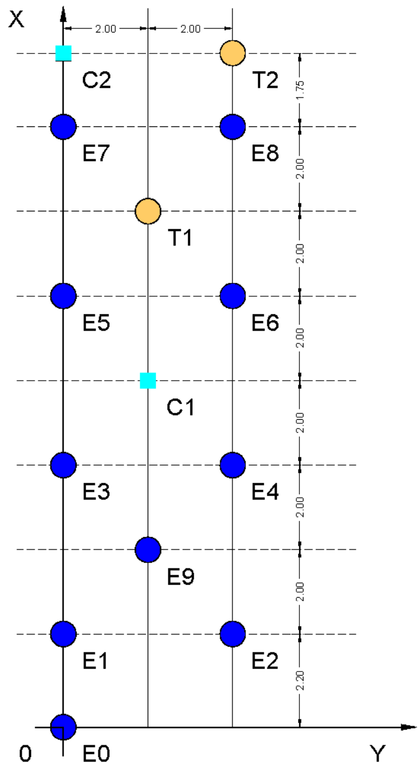

Figure 1 – Pile location.

3 Initial calculations from available in situ test data

Initially, the provided soil in situ test data were normalized by means of linear interpolations, in such way that for one specific elevation data points are available for the different in situ tests. The adopted elevation scale starts at 0 m with steps of 0,2 m.

Afterwards, statistical analyses for this specific local were performed, in order to obtain average values, standard deviations and coefficients of variation of the parameters q_t, f_t, R_f, N_{SPT}

and E_d. Further information on the local geological – geotechnical soil formation can be found in Fonseca, 2003.

4 Deterministic prediction methodology based on average soil properties

4.1 Soil resistance parameters

In the deterministic approach the soil resistance parameters under the pile base and along the pile shaft have been estimated as the average values of q_t, f_t and R_f or the best estimate of in situ test values in the nearby pile. The EXCEL spreadsheet 'Soil statistical analyses.xls' presents these average results. Also, this spreadsheet shows the soil resistance coefficients of variations (Table 1), obtained from the CPTu test results before and after the pile driving used in the probabilistic approach.

Table 1. Soil resistance coefficient of variation

	SPT	q_t	
		Before	After
Base	0,01	0,19	**0,18***
Shaft	0,30	0,32	**0,31***

* values considered in the probabilistic calculations.

In the absence of measured soil data between the pile base and the reference surface, soil parameters have been indirectly evaluated from correlation with available measured N_{SPT} data:

$$q_t = K.N_{SPT}$$

$$f_t = R_f \,.\, q_t = R_f \,.\, K \,.\, N_{SPT}$$

K= evaluated from correlations between q_t and N_{SPT} values above the pile base

4.2 Soil deformation parameters

In the deterministic approach the soil resistance parameters under the pile base and along the pile shaft have been estimated as the average values of q_t, f_t and R_f or, the closest available in situ test results. Also, the soil deformation parameter E_s under the pile base and along the pile shaft has been estimated as the average values of E_d, obtained from the DMT test results.

In the case of probabilistic approach the Table 2 shows the coefficients of variations that have been obtained from the DMT test results before and after the pile driving.

Table 2. Soil deformation coefficient of variation

	Ed	
	Before	After
Base	0,04	**0,26***
Shaft	0,20	0,30

* value considered in the probabilistic calculation.

In the absence of measured data below the pile base this value has been indirectly evaluated from available N_{SPT} data:

$$E_d = k \,.q_t$$

$$E_s = \zeta \,.\, E_d$$

k = evaluated from correlations between q_t and DMT data above pile base

ζ = empirical correction factor to take into account the pile installation process and scale effects.

The empirical correction factor ζ shown in Table 3 has been adjusted considering the dynamic load test DLT results and the DMT test results before and after the pile driving.

Table 3. Empirical correction factor for soil modulus (fine tuned values)

Pile type	ζ
Bored	0,60
Driven	2,00
Continuous flight auger	0,80

4.3 Dynamic in situ load (DLT) test analyses

The file 'capwap_results.doc' presents the summary of CAPWAP analysis of a typical blow for the piles C2, E0, E2, E6 and T2. Brazilian practice is somewhat different from that used in the available dynamic test results (DLT). According to Brazilian practice the dynamic test is performed with increasing energy blows in a test procedure called DIET (Aoki, 2000 / 2000a). EXCEL spreadsheet 'dynamic_curves.xls' presents the dynamic loading test curves (Aoki & de Mello, 1992) using a Jc damping coefficient derived from the CAPWAP analysis.

5 Pile head settlement calculation model

For a given pile, with a given length, the settlement calculation is based on the following basic assumptions derived from instrumented pile load transfer measurements:

- the average ultimate loading condition R defines a fundamental static load transfer diagram (defined support reactions forces);
- the shaft and base resistances are independent variables;
- the base resistance starts being mobilized only after all the shaft resistance has been mobilized;
- for any applied load Q greater than the ultimate shaft resistance, the difference between the applied load and the ultimate shaft resistance is carried by the pile base; in this case, the soil far from the pile-soil interface, behaves as a perfectly elastic medium;
- the shape of pile head load vs. settlement curve is defined by the van der Veen’s (1953) equation:

  $Q = R_m\ [1 - \exp(-\alpha\,\delta)]$

  Q = applied load (active force)
  R_m = van der Veens’s average ultimate pile resistance (reactive force)
  α = curve shape coefficient = $[-\ln(1 - Q/R_m)]/\delta$
  δ = pile head settlement

This formulation assures the existence of a direct link between the pile ultimate resistance definition and the shape of the predicted load vs. settlement curve.

6 Calculation steps for load vs. settlement curve prediction

6.1 Determination of the ultimate pile resistance

In this prediction the model for the calculation of the ultimate pile resistance was the method Aoki and Velloso (1975)

R_m = average ultimate resistance = PL + PP

PL = [Σ rl . U . ΔL] = average shaft resistance
PP = A . rp = average base resistance
rl = f_t /F2 = ultimate pile shaft local friction
rp = q_t/F1 = ultimate pile base resistance
A = pile base area
U = pile shaft perimeter
F1 and F2 = empirical correction factors to take into account the pile installation process, time and scale effects.

Table 4. F1 and F2 fine tuned values.

Pile type	Base resistance	Shaft friction resistance
	F1	F2
Bored	**2,00**	**3,50**
Driven	**1,25**	**1,43**
Continuous flight auger	**1,75**	**3,50**

6.2 Determination of the fundamental load transfer diagram

For an applied load R_m just before the ultimate limit state (fundamental loading condition) the normal force diagram (Aoki, 1989) along the pile shaft is given by

$N(z) = R_m – PL(z)$,

where PL(z) is the integral of the shaft resistance from the pile head up to the depth (z).

Considering the basic assumptions concerning the proposed load transfer mechanism, the normal force diagram along the pile shaft, for an applied load Q greater than the ultimate shaft resistance PL, is given by:

$N(z) = Q – PL(z)$

P_p = Q – PL = load carried by the base

In the present case, it was assumed that:

Q = 1,2 PL

6.3 Determination of pile head displacement for an applied load Q

According to Vésic (1975 the pile head displacement is

$$\delta = \delta_p + \delta_s$$

$$\delta_p = \int_C^{C+L} \frac{N(z)dz}{A.E} = \text{elastic shortening of pile shaft.}$$

C = distance between the pile base and the reference surface;
L = pile length;
A = pile transversal section area;
E = pile elasticity modulus.

Vésic (1975) suggested that the displacement of pile base section, under the action of the loads applied at the base and along the pile shaft, due to the deformations of soil layers beneath the pile base is

$$\delta_s = \delta_{s,p} + \delta_{s,1} = \text{pile base displacement}$$

The pile base displacement was evaluated using the numerical integration of Mindlin’s (1936) equations suggested by Aoki & Lopes (1975) method. This formulation requires an absolute reference system and allows the interaction of cylindrical piles and prismatic rectangular cross section piles, under the action of any known normal force diagrams.

In this way the negative forces introduced by the four neighboring anchor piles reactions in the prediction of piles C1, T1 and E9, were also taken into account, as recommended by Weele (1989). Therefore, the anchor system uplift could be evaluated for the applied load Q.

Additionally, Steinbrenner’s (1934) proposition allows the consideration of any horizontally layered soil formation.

6.4 Determination of the shape factor of load settlement curve evaluated according to Van der Veen equation

The shape factor α has been evaluated using the values of Q, R_m and δ, previously determined.

$$\alpha = \frac{-\ln(1 - Q/R_m)}{\delta}$$

6.5 Determination of the points of the static load vs. settlement curve.

The prediction of the points of the static load vs. settlement curve has been determined from the expression:

$$Q = R_m\,[1 - \exp(-\alpha\,\delta)]$$

The EXCEL spreadsheet 'deterministic_prediction.xls' presents the calculations done for the case of dynamically tested piles C2, E0, E2, E6 and T2 and the predictions for the piles C1, T1 and E9. Table 5 shows the predicted static load vs. settlement curve values for the piles C1, T1 and E9 considering the soil analysis of item 3. Figure 2 shows the corresponding load vs. settlement curves.

7 Comparison of predicted behavior under static loading condition using in situ test results with evaluated behavior using dynamic load test results.

As explained before the methodology previously described, was also used to predict the behavior under static load condition for the piles that have been dynamically tested. This procedure allowed to fine tune the empirical coefficients ζ, F1 and F2 presented in the table 3 and 4, considering the effects of different pile installation methods on soil elasticity modulus and the soil resistance.

Table 5. C1, T1 and E9 predicted static load vs. settlement at pile head.

C1		T1		E9	
Q kN	δ mm	Q kN	δ mm	Q kN	δ mm
0	0	0	0	0	0
755	2	334	2	286	2
1166	4	613	4	520	4
1389	6	844	6	711	6
1510	8	1038	8	867	8
1575	10	1199	10	995	10
1611	12	1333	12	1099	12
1630	14	1444	14	1184	14
1641	16	1538	16	1253	16
1647	18	1615	18	1310	18
1650	20	1680	20	1357	20
1651	22	1734	22	1394	22
1652	24	1778	24	1425	24
1653	26	1816	26	1451	26
1653	28	1847	28	1471	28
1653	30	1873	30	1488	30
1653	32	1894	32	1502	32
1653	34	1912	34	1513	34
1653	36	1927	36	1522	36
1653	38	1940	38	1530	38
1653	40	1950	40	1536	40
1653	42	1959	42	1541	42
1653	44	1966	44	1545	44
1653	46	1972	46	1549	46
1653	48	1977	48	1551	48
1653	50	1981	50	1553	50
1653	52	1985	52	1555	52
1653	54	1988	54	1557	54
1653	56	1990	56	1558	56
1653	58	1992	58	1559	58
1653	60	1994	60	1560	60

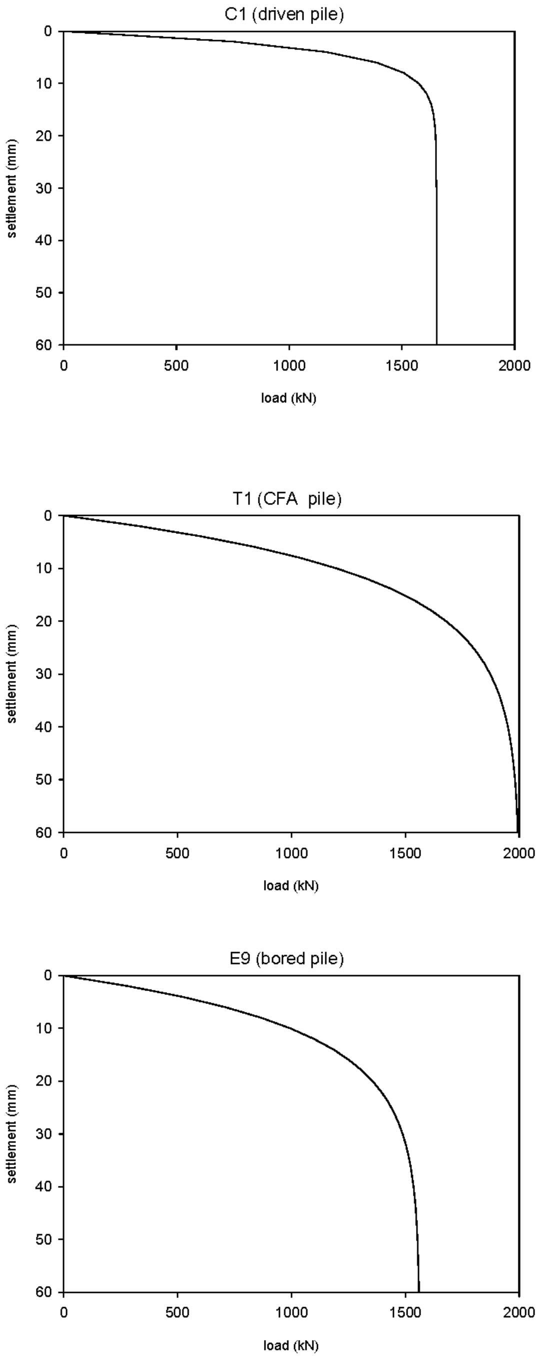

Figure 2 – Predicted load vs. settlement curves.

Table 6. E0, T2 and C2 predicted static load vs. settlement at pile head.

E0			T2			C2		
Q kN	δ mm	DLT	Q kN	δ mm	DLT	Q kN	δ mm	DLT
0	0		0	0		0	0	
228	2		314	2		587	2	
419	4		559	4		959	4	
578	6		752	6		1195	6	
711	8		903	8		1344	8	
823	10		1021	10		1439	10	
915	12		1114	12		1499	12	
993	14		1187	14		1538	14	
1058	16		1244	16		1562	16	
1112	18		1288	18		1577	18	
1157	20		1323	20		1587	20	
1195	22		1351	22		1593	22	
1227	24		1372	24		1597	24	
1253	26		1389	26		1599	26	
1275	28		1402	28		1601	28	
1294	30		1413	30		1602	30	
1309	32		1421	32		1603	32	
1322	34		1427	34		1603	34	
1333	36		1432	36		1603	36	
1342	38		1436	38		1603	38	
1349	40		1439	40		1604	40	
1355	42		1441	42		1604	42	
1361	44		1443	44		1604	44	
1365	46		1445	46		1604	46	
1369	48		1446	48		1604	48	
1372	50		1447	50		1604	50	
1374	52		1447	52		1604	52	
1376	54		1448	54		1604	54	
1378	56		1448	56		1604	56	
1380	58		1449	58		1604	58	
1381	60		1449	60		1604	60	
1146		19	1052		11	1472		5
1252		28	1010		15	1491		6
1296		36	616		5	1484		6
1310		43	1331		25	1479		7
			1430		31	1476		7
			0		0	1526		10
						1537		10

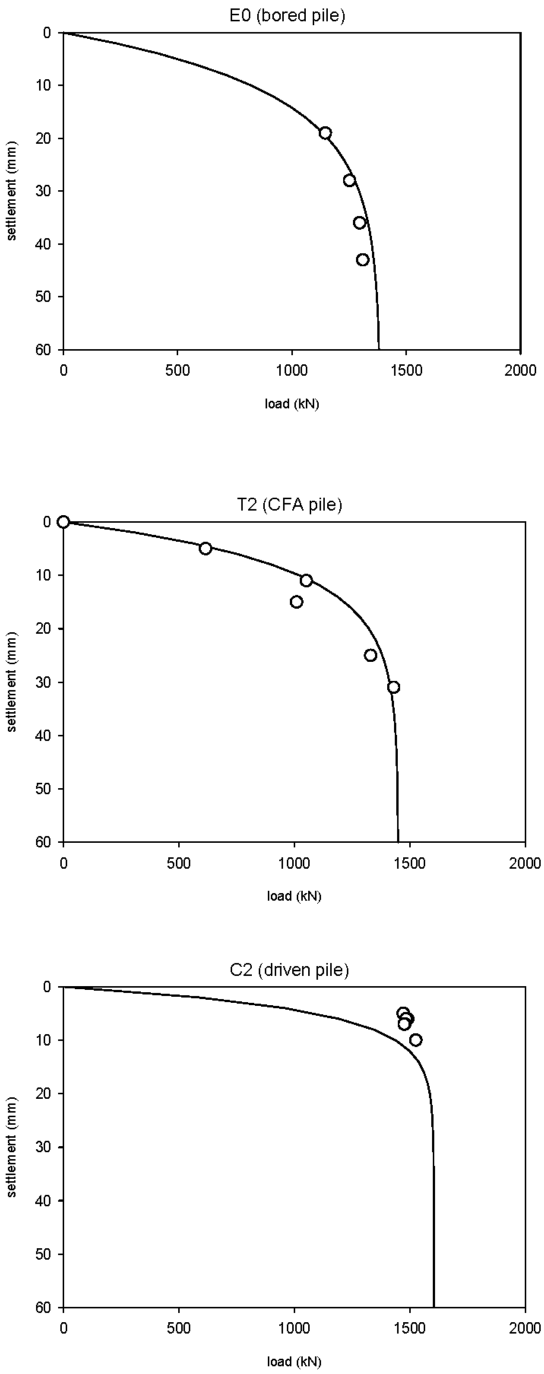

Figure 3 – Deterministic prediction of load vs. settlement curves for piles E0, T2 and C2 and the corresponding DLT results.

Table 7. E2 and E6 predicted static load vs. settlement at pile head.

E2			E6		
Q kN	δ mm	DLT	Q kN	δ mm	DLT
0	0		0	0	
1645	2		1575	2	
3037	4		2937	4	
4215	6		4116	6	
5213	8		5136	8	
6057	10		6017	10	
6771	12		6780	12	
7375	14		7440	14	
7887	16		8011	16	
8320	18		8505	18	
8687	20		8932	20	
8997	22		9302	22	
9259	24		9622	24	
9481	26		9898	26	
9669	28		10137	28	
9829	30		10344	30	
9963	32		10523	32	
10077	34		10678	34	
10174	36		10812	36	
10255	38		10928	38	
10325	40		11028	40	
10383	42		11115	42	
10432	44		11190	44	
10474	46		11255	46	
10510	48		11311	48	
10540	50		11359	50	
10565	52		11401	52	
10587	54		11438	54	
10605	56		11469	56	
10620	58		11496	58	
10633	60		11520	60	
5152		9	3072		6
6927		11	5448		9
7813		13	6485		28
8006		13	6550		12
7849		13	6519		12
8121		13	6469		12
0		0	2364		5

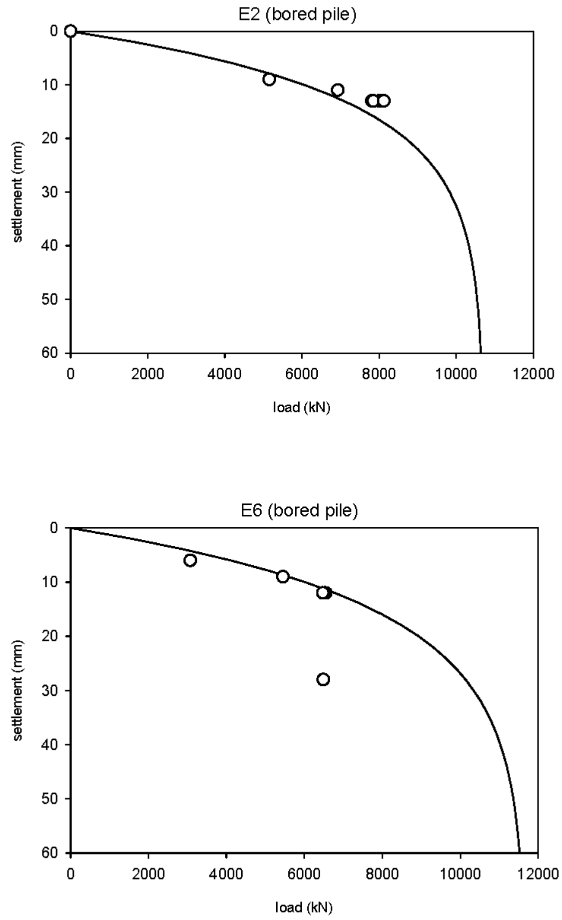

Figure 4 – Deterministic prediction of load vs. settlement curves for piles E2 and E6 and the corresponding DLT results.

8 Probabilistic prediction based on soil properties coefficients of variation

In this case the results are shown with the aid of three curves, that is to say the average curve and the upper and lower bound curves, defined by the desired *confidence interval* (Benjamin & Cornell, 1970; Lee et al., 1988). The average curve has been determined based on the average q_t, f_t and E_d results with the deterministic approach calculation, as described in steps 2 to 7. Therefore, the following independent sources of variability have been taken into account in this approach:

- Pile type and pile length;
- The desired *confidence interval* for the prediction (CI);

- The soil resistance variability given by the q_t coefficient of variation (CVLR) values along the length of the pile shaft;
- The soil resistance variability represented by the q_t coefficient of variation (CVBR) values under the pile base;
- The soil deformation variability represented by the E_d coefficient of variation (CVSM) values bellow the pile base;

The pile material resistance and deformation modulus have been considered constant, so that the elastic pile shortening remains constant for a given applied load Q.

Assuming that the base and shaft resistances probability density functions are represented by Gaussian random mutually independent variables, the standard deviation of the total ultimate resistance R_m is given by

$$\sigma_R = (\sigma_L^2 + \sigma_B^2)^{0,5}$$

σ_L = shaft resistance standard deviation;

σ_B = base resistance standard deviation.

The corresponding coefficients of variation are

CVLR = σ_L / PL = shaft resistance coefficient of variation;

CVBR = σ_B / PP = base resistance coefficient of variation.

The combined ultimate resistance coefficient of variation is

CVUR = σ_R / R_m = coefficient of variation of ultimate resistance.

The probability area *p* corresponding to a given confidence interval CI is

$$p = (1\text{-CI})$$

The corresponding β value can be calculated by the EXCEL spreadsheet expression

$$\eta = \text{-NORMINV}(p,0,1)$$

The corresponding intervals of the ultimate resistance values are then calculated as

$$R_{upper} = R_m (1 + \beta \,.\, \text{CVUR})$$

$$R_{lower} = R_m (1 - \beta \,.\, \text{CVUR})$$

The settlement corresponding to the applied load Q is

$$\delta = \delta_p + \delta_s$$

The elastic pile shortening δ_p remains constant. The pile base settlement δ_s values, corresponding to a given applied load Q, for the upper and lower soil modulus values, are given by

$$\delta_{s,\,min} = (1 + \beta \,.\, \text{CVSM}).\delta_s$$

$$\delta_{s,\,max} = (1 - \beta \,.\, \text{CVSM}).\delta_s$$

δ_s = settlement corresponding to the mean soil modulus below the pile base.

CVSM = soil modulus coefficient of variation

The upper load vs. settlement curve is given by the Van der Veen expression, considering the R_{upper}, Q and $\delta_{s,min}$ values. In the same way, the lower load vs. settlement curve has taken as parameters R_{lower}, Q and $\delta_{s,max}$ values.

The EXCEL spreadsheet file 'probabilistic_prediction.xls' shows the calculation results corresponding to a confidence interval CI = 95% and the soil coefficient of variation found in the tables 1, 2 and 3, for bored, driven and CFA piles with length of 6 m.

- CVLR = 0,31
- CVBR = 0,18
- CVSM = 0,26

Greater the chosen confidence interval (CI) or greater the soil parameter coefficient of variation (CV), larger will be the scatter around the average deterministic curve. Any desired independent variable combination could be considered.

9 Tables and curves corresponding to the probabilistic prediction approach

Table 8 and Figure 5 shows the prediction results obtained according to item 10.

Table 8. Probabilistic prediction of load vs. settlement curves for driven, CFA and bored piles

Driven Pile						CFA Pile						Bored Pile					
Average Curve		Upper Curve		Lower Curve		Average Curve		Upper Curve		Lower Curve		Average Curve		Upper Curve		Lower Curve	
Q kN	δ mm	Q kN	δ mm	Q kN	δ mm	Q kN	δ mm	Q kN	δ mm	Q kN	δ mm	Q kN	δ mm	Q kN	δ mm	Q kN	δ mm
0	0	0	0	0	0	0	0	0	0	0	0	0	0	0	0	0	0
699	2	761	1	108	1	370	2	709	2	203	2	270	2	293	1	38	1
1082	4	1547	3	438	3	647	4	1149	4	368	4	486	4	739	3	177	3
1292	6	1861	5	649	5	855	6	1422	6	502	6	660	6	1046	5	296	5
1407	8	1986	7	783	7	1011	8	1591	8	611	8	799	8	1258	7	398	7
1469	10	2036	9	869	9	1128	10	1697	10	700	10	910	10	1403	9	485	9
1504	12	2056	11	924	11	1216	12	1762	12	773	12	1000	12	1504	11	559	11
1523	14	2065	13	959	13	1282	14	1803	14	831	14	1071	14	1573	13	622	13
1533	16	2068	15	982	15	1331	16	1828	16	879	16	1129	16	1621	15	676	15
1539	18	2069	17	996	17	1368	18	1844	18	918	18	1175	18	1654	17	723	17
1542	20	2070	19	1005	19	1396	20	1853	20	950	20	1212	20	1677	19	762	19
1543	22	2070	21	1011	21	1416	22	1859	22	976	22	1241	22	1692	21	796	21
1544	24	2070	23	1014	23	1432	24	1863	24	997	24	1265	24	1703	23	825	23
1545	26	2070	25	1017	25	1444	26	1865	26	1014	26	1284	26	1711	25	850	25
1545	28	2070	27	1018	27	1452	28	1867	28	1028	28	1299	28	1716	27	871	27
1545	30	2070	29	1019	29	1459	30	1868	30	1039	30	1311	30	1719	29	889	29
1545	32	2070	31	1020	31	1464	32	1868	32	1048	32	1321	32	1722	31	904	31
1545	34	2070	33	1020	33	1468	34	1869	34	1055	34	1329	34	1723	33	917	33
1545	36	2070	35	1021	35	1470	36	1869	36	1062	36	1335	36	1725	35	928	35
1545	38	2070	37	1021	37	1472	38	1869	38	1067	38	1340	38	1725	37	938	37
1545	40	2070	39	1021	39	1474	40	1869	40	1071	40	1344	40	1726	39	946	39
1545	42	2070	41	1021	41	1475	42	1869	42	1074	42	1348	42	1726	41	953	41
1545	44	2070	43	1021	43	1476	44	1869	44	1076	44	1350	44	1727	43	959	43
1545	46	2070	45	1021	45	1477	46	1869	46	1079	46	1352	46	1727	45	964	45
1545	48	2070	47	1021	47	1477	48	1869	48	1080	48	1354	48	1727	47	969	47
1545	50	2070	49	1021	49	1478	50	1869	50	1082	50	1355	50	1727	49	972	49
1545	52	2070	51	1021	51	1478	52	1869	52	1083	52	1356	52	1727	51	976	51
1545	54	2070	53	1021	53	1478	54	1869	54	1084	54	1357	54	1727	53	978	53
1545	56	2070	55	1021	55	1478	56	1869	56	1085	56	1358	56	1727	55	981	55
1545	58	2070	57	1021	57	1478	58	1869	58	1085	58	1359	58	1727	57	983	57
1545	60	2070	59	1021	59	1478	60	1869	60	1086	60	1359	60	1727	59	984	59

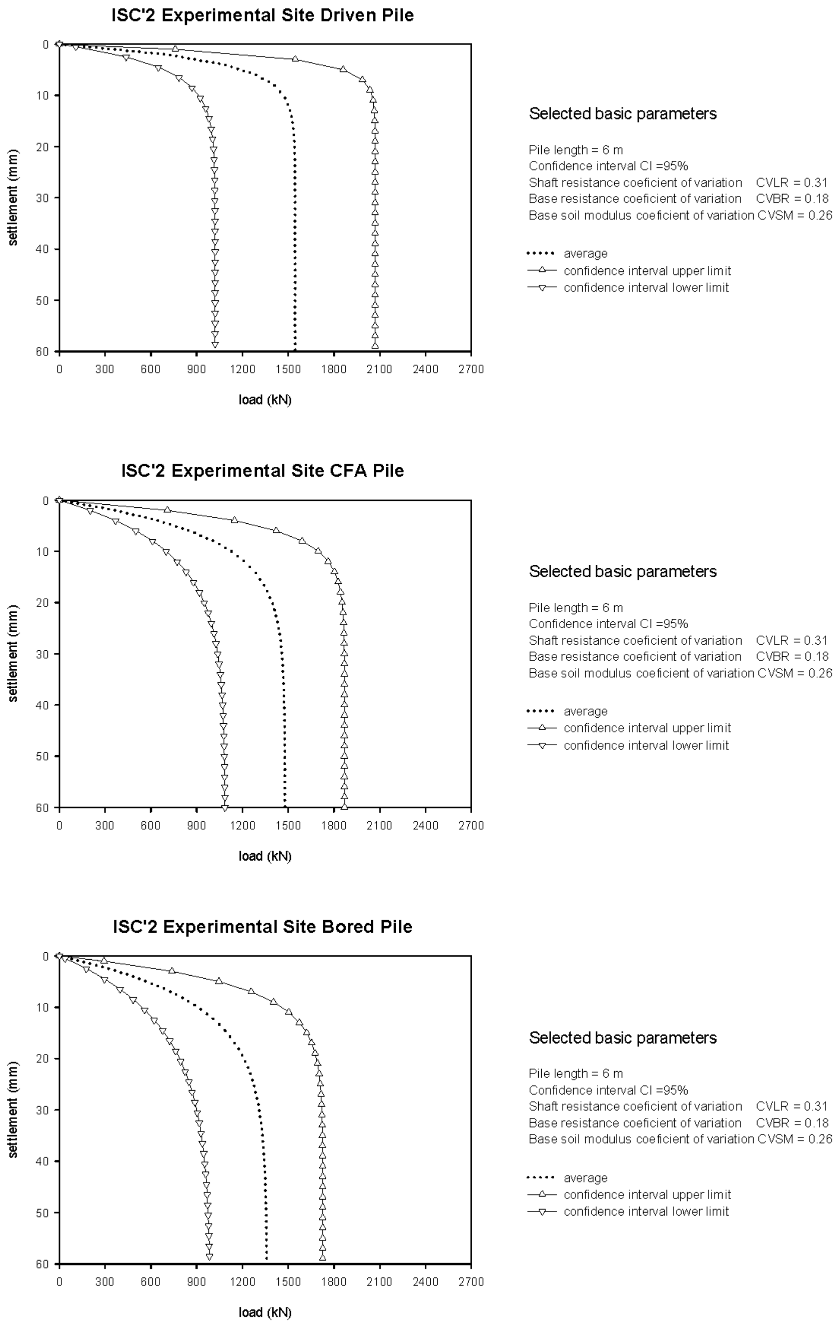

Figure 5 – Probabilistic prediction of the load vs. settlement curves for the driven, CFA and bored piles

10 Allowable bearing capacity and factor of safety

10.1 Direct interdependence of failure probability, factor of safety and allowable load

This prediction suggests that the allowable bearing capacity and factor of safety could be referred only to a given set of piles in a given site. Obviously, factor of safety can also be referred to an individual pile but this procedure has no statistical meaning.

The traditional pile foundation design methods consider that the factor of safety is independent of the failure probability. As a consequence, the failure probability remains unknown. The probabilistic definition of allowable bearing capacity demands the knowledge of the interdependence function relating the global factor of safety and the *associated failure probability.*

According to Ang and Tang (1984) the margin of safety is defined as

Z = margin of safety = $(R_m - S_m) = \beta.\sigma_Z$

R_m = average resistance (axial ultimate pile resistance);

S_m = average load action effect (internal axial compressive force);

β = reliability index;

$\sigma_Z = (\sigma_S^2 + \sigma_R^2)^{0,5}$

σ_S = ultimate resistance standard deviation;

σ_R = compressive force standard deviation.

$v_S = \sigma_S / R_m$ = axial compressive force coefficient of variation

$v_R = \sigma_R / S_m$= axial ultimate resistance coefficient of variation

In this case the central factor of safety is

$F_S = R_m / S_m$ = central safety factor

Using the above Ang and Tang (1984) definitions, the factor of safety can be obtained as follows

$$F_S = [\,1 + \beta\,(v_S^2 + v_R^2 - \beta^2 v_S^2 v_R^2)^{0,5}\,] / (1- \beta^2 v_R^2)$$

This equation establishes the relationship between the central factor of safety and the *probability of failure* (p_F), represented by the reliability index β. The *probability of failure* (p_F) can be determined by the EXCEL formula

p_F =1-NORMDIST(β,0,1,TRUE)

The traditional allowable load P_{all} could be taken as the *average* or the *characteristic* values of the load action effect (internal axial compressive force). Considering the average value (Aoki, 2002 and Aoki et al., 2002a) results

$P_{all} = R_m - \beta.\sigma_Z$

Particular cases are

$v_S = 0$ = constant force

$F_S = [1 / (1-\beta.\,v_R)] \rightarrow \quad P_{all} = R_m\,(1-\beta.\,v_R)$

$v_R = 0$ = constant resistance

$F_S = [1 + \beta.\,v_S] \quad \rightarrow \quad P_{all} = R_m / (1+\beta.\,v_S)$

The variability of several pile types in several case histories has been analyzed by Silva (2003).

The reliability index β has been derived by Cardoso & Fernandes (2001), and is given by

$$\beta = (1-S_m/R_m) /[v_R^2+ (S_m/R_m)^2 v_S^2]^{0,5}$$

Considering the above safety of factor definition, this expression can be rewritten as

$$\beta = (1- 1/ F_S) / [v_R^2 + (1/ F_S)^2 v_S^2]^{0,5}$$

It can be concluded that the suggested approach for pile design, using this allowable load concept can be used in practice. Following, the design steps are described:

- Determination of the probability density function (PDF) of ultimate resistances (R) and of forces generated by the load action effects (S);
- Selection of the desired failure probability (p_F) and the corresponding β value;
- Determination of the corresponding allowable load and associated safety of factor
- Adequacy verification of this safety of factor against the minimum local foundation code of practice requirements.

Note that it is not possible to choose an arbitrarily fixed central safety factor once it is dependent on the fixed failure probability and specific PDFs of ultimate resistances (R) and load action effects (S).

10.2 Application example of direct interdependence of failure probability, factor of safety and allowable load

This direct interdependence can be presented in the form of graphs, relating failure probability, factor of safety and allowable load. As an application example, let be considered the conditions presented in Figure 5:

- Determination of the probability density function (PDF) of ultimate resistances:

Pile type	R_m (kN)	σ_R (kN)	v_R
Driven pile	1545	319	0,206
CFA pile	1479	237	0,161
Bored pile	1361	223	0,164

- Determination of the probability density function (PDF) of load action effects: in this case it is assumed that the load action effect is deterministic, and as a consequence $v_S = 0$
- Selection of the desired failure probability (p_F) and the corresponding β value: in this case it is adopted the range $10^{-1} \geq p_F \geq 10^{-6}$
- Determination of the safety of factor and the corresponding allowable load:

$$F_S = [1 / (1-\beta .\, v_R)] \rightarrow \quad P_{all} = R_m (1-\beta .\, v_R)$$

- Adequacy verification of this safety of factor against the minimum local foundation code of practice requirements.

Table 9. Interdependence of failure probability, factor of safety and allowable load for the ISC'2 Experimental Site

Driven			CFA			Bored		
pF	FS	P_{all} (kN)	pF	FS	P_{all} (kN)	pF	FS	P_{all} (kN)
5.00E-01	1.000	1545	5.00E-01	1.000	1479	5.00E-01	1.000	1361
3.33E-01	1.098	1408	3.33E-01	1.074	1376	3.33E-01	1.076	1265
2.50E-01	1.162	1330	2.50E-01	1.121	1319	2.50E-01	1.124	1211
2.00E-01	1.210	1277	2.00E-01	1.156	1279	2.00E-01	1.160	1173
1.67E-01	1.249	1237	1.67E-01	1.184	1249	1.67E-01	1.188	1145
1.43E-01	1.282	1205	1.43E-01	1.207	1225	1.43E-01	1.212	1123
1.25E-01	1.311	1179	1.25E-01	1.227	1206	1.25E-01	1.232	1105
1.11E-01	1.337	1156	1.11E-01	1.244	1189	1.11E-01	1.250	1089
1.00E-01	1.359	1137	1.00E-01	1.259	1174	1.00E-01	1.265	1075
5.00E-02	1.514	1021	5.00E-02	1.359	1088	5.00E-02	1.368	994
3.33E-02	1.609	961	3.33E-02	1.417	1043	3.33E-02	1.429	952
2.50E-02	1.679	921	2.50E-02	1.459	1013	2.50E-02	1.472	924
2.00E-02	1.735	891	2.00E-02	1.492	991	2.00E-02	1.506	903
1.67E-02	1.783	867	1.67E-02	1.519	973	1.67E-02	1.535	887
1.43E-02	1.824	847	1.43E-02	1.542	959	1.43E-02	1.559	873
1.25E-02	1.860	831	1.25E-02	1.562	946	1.25E-02	1.580	862
1.11E-02	1.893	816	1.11E-02	1.580	936	1.11E-02	1.598	851
1.00E-02	1.923	804	1.00E-02	1.596	926	1.00E-02	1.615	843
5.00E-03	2.134	724	5.00E-03	1.705	867	5.00E-03	1.729	787
3.33E-03	2.271	680	3.33E-03	1.772	834	3.33E-03	1.799	756
2.50E-03	2.376	651	2.50E-03	1.821	812	2.50E-03	1.850	736
2.00E-03	2.462	628	2.00E-03	1.859	795	2.00E-03	1.891	720
1.67E-03	2.535	610	1.67E-03	1.892	782	1.67E-03	1.925	707
1.43E-03	2.600	595	1.43E-03	1.919	770	1.43E-03	1.954	696
1.25E-03	2.657	582	1.25E-03	1.944	761	1.25E-03	1.980	687
1.11E-03	2.710	570	1.11E-03	1.965	752	1.11E-03	2.003	679
1.00E-03	2.759	560	1.00E-03	1.985	745	1.00E-03	2.024	672
5.00E-04	3.113	496	5.00E-04	2.120	697	5.00E-04	2.167	628
3.33E-04	3.356	461	3.33E-04	2.205	671	3.33E-04	2.257	603
2.50E-04	3.547	436	2.50E-04	2.267	652	2.50E-04	2.324	585
2.00E-04	3.708	417	2.00E-04	2.317	638	2.00E-04	2.378	572
1.67E-04	3.849	402	1.67E-04	2.359	627	1.67E-04	2.423	562
1.43E-04	3.974	389	1.43E-04	2.395	617	1.43E-04	2.462	553
1.25E-04	4.091	378	1.25E-04	2.428	609	1.25E-04	2.497	545
1.11E-04	4.198	368	1.11E-04	2.457	602	1.11E-04	2.528	538
1.00E-04	4.298	360	1.00E-04	2.483	596	1.00E-04	2.557	532
5.00E-05	5.066	305	5.00E-05	2.665	555	5.00E-05	2.754	494
3.33E-05	5.628	275	3.33E-05	2.778	532	3.33E-05	2.878	473
2.50E-05	6.124	252	2.50E-05	2.868	516	2.50E-05	2.976	457
2.00E-05	6.548	236	2.00E-05	2.937	503	2.00E-05	3.052	446
1.67E-05	6.988	221	1.67E-05	3.003	492	1.67E-05	3.124	436
1.43E-05	7.281	212	1.43E-05	3.044	486	1.43E-05	3.170	429
1.25E-05	7.712	200	1.25E-05	3.100	477	1.25E-05	3.232	421
1.11E-05	8.071	191	1.11E-05	3.144	470	1.11E-05	3.281	415
1.00E-05	8.330	186	1.00E-05	3.174	466	1.00E-05	3.314	411
5.00E-06	11.197	138	5.00E-06	3.435	430	5.00E-06	3.605	377
3.33E-06	14.265	108	3.33E-06	3.621	408	3.33E-06	3.815	357
2.50E-06	16.022	96	2.50E-06	3.701	400	2.50E-06	3.906	348
2.00E-06	21.256	73	2.00E-06	3.872	382	2.00E-06	4.101	332
1.67E-06	21.256	73	1.67E-06	3.872	382	1.67E-06	4.101	332
1.43E-06	31.571	49	1.43E-06	4.061	364	1.43E-06	4.317	315
1.25E-06	31.571	49	1.25E-06	4.061	364	1.25E-06	4.317	315
1.11E-06	61.332	25	1.11E-06	4.268	346	1.11E-06	4.557	299
1.00E-06	61.332	25	1.00E-06	4.268	346	1.00E-06	4.557	299

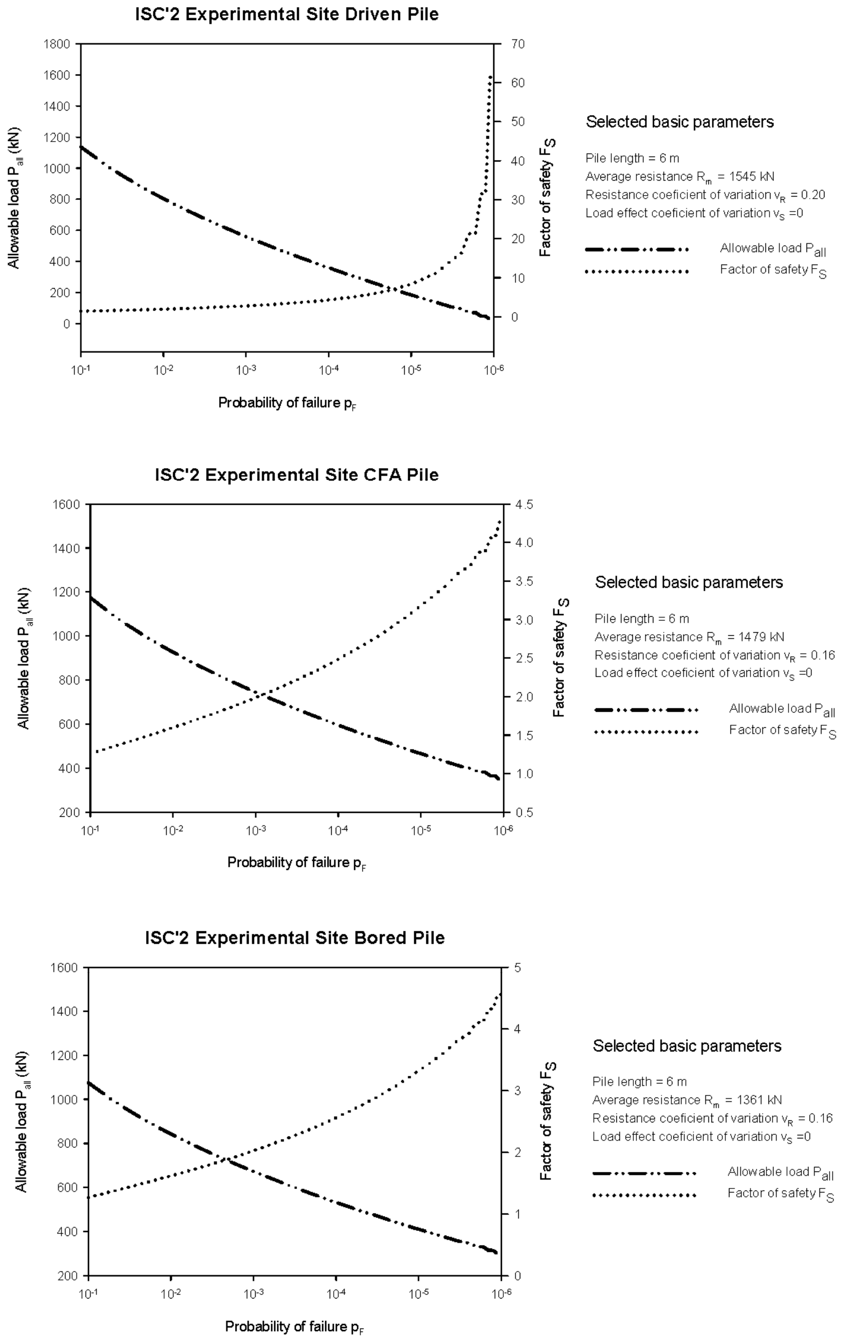

Figure 5 – Interdependence of failure probability, factor of safety and allowable load for the ISC’2 Experimental Site

As an example application of the previous figure, assuming that p_F is 1/1000, from Figure 5 it can be obtained the factors of safety and the allowable loads, as shown in Table 10.

Table 10. ISC'2 Experimental Site allowable load, and safety factors for $p_F = 10^{-3}$.

Pile type	Section	Dimension m	Length m	R_m kN	σ_R kN	v_R	P_{all} kN	F_S
Bored	Circular	0,6	6,00	1361	223	0,164	672	2,02
Driven	Square	0,35	6,00	1545	319	0,206	560	2,76
CFA	Circular	0,60	6,00	1479	237	0,161	745	1,98

If the ISC'2 Experimental Site were in Brazil, the factors of safety would be considered satisfactory, according to the Brazilian Foundation Code of Practice NBR6122/1996.

11 Acknowledgements

The authors would like to express their gratitude to the Geotechnical Engineering Department faculty, as well to the graduate students, for their valuable and pertinent discussions about this relevant research topic. It is expected that this international prediction work may contribute to change the present foundation design culture, based on solely factor of safety.

12 References

Ang, A.H.S; Tang, W.H. (1984). Probability concepts in engineering planning and design: decision, risk and reliability. New York. John Wiley, Vol.2.

Aoki, N.; Velloso, D.A. (1975). An Approximate Method to Estimate the Bearing Capacity of Piles. 5th Pan-American Conference on Soil Mechanics and Foundation Engineering, Buenos Aires, Argentina, Tome 1, 367-376.

Aoki, N.; Lopes, F. R. (1975) Estimating Stress and Settlement Due to Deep Foundation. 5th Pan-American. Conference on Soil Mechanics and Foundation Engineering, Buenos Aires, Argentina, Tome 1, 377-386.

Aoki, N. (1989). Prediction of the behavior of vertical driven pile under static and dynamic conditions. Technical Committee on Pile driving. International Society for Soil Mechanics and Foundation Engineering: Final Report of the Questionnaire Survey. Drivability of Piles, Vol. 2, 43-100.

Aoki, N.; de Mello, V.F.B. (1992). Dynamic loading test curves. Ed. Frans B.J. Barends, Application of Stress Wave Theory to Piles. Proceedings of the Fourth International Conference on the Application of Stress-Wave Theory to Piles.

Aoki, N. (2000). Keynote Lecture: Improving the reliability of pile bearing capacity by the dynamic increasing energy (DIET). Sixth International Conference on Stress Theory to Piles, Application of Stress Theory to piles – Quality Assurance on Land and Offshore Piling, Balkema, 635-650

Aoki, N. (2000a). Case histories, pile set-up and correlations between test methods-prediction reliability. Ground Engineering. September, 36.

Aoki, N. (2002). Allowable load and failure probability of pile foundations. C&T Military Revue of Science and Technology, Rio de Janeiro, 48-64 (in Portuguese).

Aoki, N.; Cintra, J.C.A.; Menegotto, M.L. (2002a). Safety and reliability of deep foundations. 8th. Congresso Nacional de Geotecnia, Lisboa, 797-806 (in Portuguese).

Benjamin, J.R.; Cornell, C.A. (1970). Probability, Statistics and Decision for Civil Engineers. McGraw-Hill, Inc., 387-396.

Cardoso, A.S., Fernandes, M.M. (2001). Characteristic values of ground parameters and probability of failure in design according to Eurocode 7. Géotechnique 51, No. 6, 519-531.

Fonseca, A.V. (2003). Characterizing and deriving engineering properties of a saprolitic soil from granite, in Porto. Characterization and Engineering Properties of Natural Soils – Tan et al. (eds.). Swets & Zeitlinger, Lisse, ISBN 90 5809 537 1.

Lee, I.K.; White, W.; Ingles, O.G. (1983). Geotechnical Engineering. Chapter 2: Soil Variability, Pitman, 57-89.

Mindlin, R.D. (1936). Force at a Point in the Interior of a Semi-infinite Solid. Physics, Vol.7, No. 5, 195-202.

Steinbrenner,W.(1934). Tafeln zur Stzungsberechnung, Die Strasse, Vol. 1, 121.

Silva, F.C. (2003). Safety and reliability analyses of deep foundations on piles. Dissertation (M. Sc). São Carlos School of Engineering - São Paulo University, Vol.1. 236p (In Portuguese).

Veen, C.V. (1953) The Bearing Capacity of a Pile. Proceedings 3rd International Conf. on Soil Mechanics and Found. Eng., Vol. 2, Switzerland.

Vésic, A.S. (1975). Principles of Pile Foundation Design. Duke University, School of Engineering, Soil Mechanics Series, No. 38.

Weele, A.F. Van (1989) Special Lecture E: Prediction versus Performance, Proceedings of the Twelfth International Conference on Soil Mechanics and Foundation Engineering, Rio de Janeiro, Vol. 4, 2259-2273.